Deposition ice nucleation on soot at temperatures relevant for the lower troposphere

Magdalena Dymarska,[1] Benjamin J. Murray,[1] Limin Sun,[1] Michael L. Eastwood,[1] Daniel A. Knopf,[1] and Allan K. Bertram[1]

Received 26 August 2005; revised 7 November 2005; accepted 1 December 2005; published 25 February 2006.

[1] The ice nucleating efficiency of many important atmospheric particles remains poorly understood. Here we investigate the ice nucleation properties of a range of soot types including soot that has been treated with atmospherically relevant amounts of ozone. We focus on deposition nucleation below water saturation and at temperatures ranging from 243 to 258 K. For our experimental conditions, ice nucleation never occurred at temperatures above 248 K and below water saturation. Below 248 K, ice occasionally formed in our experiments with no indication of the formation of water droplets prior to ice formation. However, even at these temperatures the relative humidity with respect to ice (RH_i) was close to water saturation when ice nucleation was observed, suggesting water nucleation may have occurred first followed by ice nucleation during the condensation process. We also performed a complimentary set of experiments where we held soot particles at 248 K and $RH_i = 124 \pm 4\%$, which is just below water saturation, for a period of 8 hours. From these measurements we calculated an upper limit of the heterogeneous ice nucleation rate coefficient of 0.1 cm^{-2} s^{-1}. If the number of soot particles is 1.5×10^5 L^{-1} in the atmosphere (which corresponds to urban-influenced rural areas), then the number of ice particles produced below water saturation at these conditions is at most 0.1 particles L^{-1} on the basis of our upper limit. We conclude from our studies that deposition nucleation of ice on most types of soot particles is not important in the Earth's troposphere above 243 K and below water saturation.

Citation: Dymarska, M., B. J. Murray, L. Sun, M. L. Eastwood, D. A. Knopf, and A. K. Bertram (2006), Deposition ice nucleation on soot at temperatures relevant for the lower troposphere, *J. Geophys. Res.*, *111*, D04204, doi:10.1029/2005JD006627.

1. Introduction

[2] Clouds play an important role in climate by scattering and absorbing radiation. Currently, clouds and their interaction with aerosol particles provide some of the greatest uncertainties in predictions of climate change [*Intergovernmental Panel on Climate Change*, 2001]. This is, in large part, because the properties of clouds and their formation processes are poorly understood, particularly the properties and formation processes of mixed phase clouds and ice clouds [*Penner et al.*, 2001].

[3] Ice particles can form in the atmosphere when ice homogeneously nucleates in aqueous particles or ice heterogeneously nucleates on solid particles. Heterogeneous freezing can occur in four different modes: deposition nucleation, condensation freezing, immersion freezing, and contact freezing [*Vali*, 1985]. Deposition nucleation occurs when vapor absorbs onto a solid surface and is transformed into ice. Condensation freezing refers to the sequence of events whereby cloud condensation initiates freezing of the condensate. Immersion freezing occurs when ice nucleates on a solid particle immersed in a liquid droplet, and contact freezing occurs when a solid particle collides with a liquid droplet, resulting in ice nucleation [*Pruppacher and Klett*, 1997; *Vali*, 1985]. In practice, the distinction between condensation freezing and immersion freezing is not always clear. In order to understand the role that mixed phase and ice clouds play in the atmosphere, these formation processes must be understood and quantified. At temperatures between 273 and 238 K ice formation necessarily occurs by heterogeneous freezing. This temperature range is more relevant for the lower troposphere. As pointed out by *Vali* [1996] in a review on ice nucleation, the origin of ice in lower-tropospheric clouds is not resolved, and it remains a question of great importance and in need of new efforts. This paper focuses on ice nucleation in the deposition mode at temperatures relevant for the lower troposphere.

[4] Soot particles are ubiquitous in the Earth's troposphere, [*Finlayson-Pitts and Pitts*, 2000; *Heintzenberg*, 1989; *Seinfeld and Pandis*, 1998] and ice core measurements suggest that their concentrations in the atmosphere have increased from preindustrialization to modern times [*Lavanchy et al.*, 1999]. If soot particles are effective ice nuclei (IN), they have the potential to significantly impact

[1]Department of Chemistry, University of British Columbia, Vancouver, British Columbia, Canada.

0148-0227/06/2005JD006627$09.00

Table 1. Physical Characteristics of the Soot Types Investigated in This Study

Type of Soot	Volatiles,[a] %	BET-Surface Area,[b] $m^2\ g^{-1}$	C%	H%	O%	N%
N-hexane soot: diffusion flame	ND	89 ± 2	87 to 95	1.6 to 1.2	11 to 6	ND
N-hexane soot: air/fuel = 0.53	ND	100 ± 2	ND	ND	ND	ND
N-hexane soot: air/fuel = 2.4	ND	156 ± 11	ND	ND	ND	ND
Lamp Black 101	1	20	98.5	0.4	0.4	0.1
Degussa FW2 (Channel Black)	17	460	88	1.1	9.9	0.7
Printex 40 (Furnace Black)	0.9	90	ND	ND	ND	ND

[a]Volatiles were determined by heating a sample in a muffle furnace for 7 min at 950°C.
[b]BET (Brunauer, Emmett, and Teller) surface area was calculated from the N_2 absorption isotherms recorded at 77 K.

the Earth's climate indirectly by changing the properties and lifecycle of mixed phase and ice clouds on a global scale [*DeMott*, 2002; *DeMott et al.*, 1997; *Gierens*, 2003; *Jensen and Toon*, 1997; *Lohmann*, 2002; *Lohmann and Feichter*, 2005]. In the lower troposphere, an increase in soot particles may lead to more frequent glaciation of supercooled clouds and increase the amount of precipitation via the ice phase. Further, this may reduce the cloud cover in the lower troposphere and result in increased absorption of solar radiation [*Lohmann*, 2002; *Lohmann and Feichter*, 2005]. However, this aerosol indirect effect on climate is uncertain, in part, because the conditions at which ice nucleates on soot particles in the atmosphere are not known.

[5] At present there have only been a limited number of laboratory studies on the ice nucleating ability of soot particles at temperatures above 238 K [*DeMott*, 1990; *Diehl and Mitra*, 1998; *Gorbunov et al.*, 2001]. Types of soot particles investigated in the previous studies include particles produced from the combustion of acetylene [*DeMott*, 1990], kerosene [*Diehl and Mitra*, 1998], benzene and toluene [*Gorbunov et al.*, 2001], as well as soot produced by thermal decomposition of benzene [*Gorbunov et al.*, 2001]. The previous measurements suggest that soot particles are potentially important ice nuclei in the atmosphere. However, more work is still needed to understand ice nucleation on soot over this temperature range (above 238 K). For example, the ice nucleating ability as a function of relative humidity below water saturation needs to be investigated at these temperatures, since the previous studies mainly focused on ice nucleation at or slightly above liquid water saturation.

[6] In the following we investigate ice nucleation on soot particles focusing on deposition nucleation below water saturation and at temperatures ranging from 243 K to 258 K. Experiments were done as a function of both temperature and relative humidity. For these studies we used several different types of soot particles and carbon black particles with a range of physical and chemical properties. We also carried out experiments to determine if the oxidization of soot particles increases their ability to act as ice nuclei. It has previously been speculated that oxidation of soot by ozone in the atmosphere will increase the ice nucleation ability of soot particles [*Gorbunov et al.*, 2001]. As a test of this hypothesis, we exposed Lamp Black 101, a commercial carbon black, to ozone for extended periods of time, and then tested its ice nucleation ability in the deposition mode. Finally, for comparison purposes, we investigated the ice nucleating ability of kaolinite using similar experimental parameters as the experiments involving soot. Kaolinite is believed to be a significant component of mineral dust in the atmosphere [*Glaccum and Prospero*, 1980; *Pye*, 1987].

2. Methods

[7] The different soots and carbon blacks used in these studies are listed in Table 1. Three different samples of n-hexane soot were provided by Dwight M. Smith, University of Denver. The first sample was produced by burning n-hexane under ambient conditions in an open vessel, resulting in a diffusion flame. The second and third samples were generated using an apparatus designed for producing premixed flames with variable oxidant to fuel ratios. It has been shown that there is a linear relationship between the state of soot surface oxidation and the air to fuel ratio [*Chughtai et al.*, 2002]. The International Steering Committee for Black Carbon Reference Materials has recommended using n-hexane soot as a model for soot in the atmosphere because a large amount of soot characteristics and reactivity data already exists in the scientific literature on this type of soot and because of the option to vary the n-hexane soot properties by varying the combustion conditions (http://www.du.edu/~dwismith/bcsteer.html). Properties of n-hexane soot have been documented by Smith and coworkers [*Akhter et al.*, 1985; *Chughtai et al.*, 2002]. Lamp Black 101, Degussa FW2 (which is a channel type black), and Printex 40 (which is a furnace type black) are commercial carbon blacks. Degussa FW2 is posttreated with NO_2 and has been used in the past in laboratory heterogeneous chemistry studies [see for example *Choi and Leu*, 1998; *Disselkamp et al.*, 2000; *Tabor et al.*, 1994]. Lamp Black 101 is essentially nonvolatile at 1223 K and has been used in the past for ice nucleation studies [*DeMott et al.*, 1999]. Neither Lamp Black 101 nor Printex 40 are posttreated. Relevant properties of these soot particles and carbon blacks are summarized in Table 1. The kaolinite particles used in our experiments were purchased from Fluka Chemika (purum; natural grade).

[8] The apparatus used in these studies consisted of an optical microscope coupled to a flow cell in which the relative humidity could be accurately controlled. The flow cell, which is shown in Figure 1, was similar to the one used previously to measure deliquescence and crystallization of supermicron organic and mixed organic-inorganic particles [*Pant et al.*, 2004; *Parsons et al.*, 2004a, 2004b]. In the current experiments soot or kaolinite particles were deposited on the bottom surface of the flow cell; the relative humidity with respect to ice (RH_i) inside the cell was increased, and the conditions under which water droplets or ice crystals formed were determined with a reflected light microscope (Zeiss Axiotech 100) equipped with a 10x

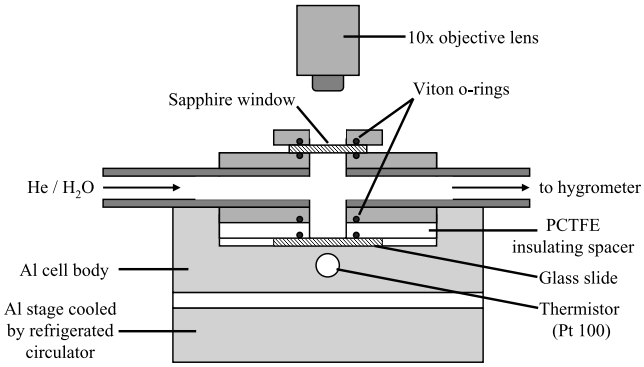

Figure 1. Flow cell and location of microscope objective (Al = aluminum and PCTFE = polychlorotrifluoroethylene).

objective lens. The RH_i over the particles was controlled by continuously flowing a mixture of dry and humidified He through the flow cell.

[9] The bottom surface of the flow cell, which supported the particles, consisted of a glass cover slide treated with dichlorodimethylsilane (DCMS) to make a hydrophobic layer, which reduced the probability of ice nucleation directly on the surface. Prior to the treatment with DCMS the glass slide was thoroughly cleaned in a pirahna solution (3:1 mixture by volume of sulfuric acid and hydrogen peroxide), rinsed in high-purity water (distilled water further purified with a Millipore system) and methanol (HPLC grade), and any remaining contaminant particles removed with a dry ice cleaning system (Sno Gun-II™, Va-Tran Systems). The treatment with DCMS involved placing the slides in an airtight chamber together with 2–3 droplets of DCMS solution (Fluka, 5% DCMS in heptane). The slides were not in direct contact with the droplets, rather the DCMS coated the glass slides via vapor deposition.

[10] All samples were prepared and the flow cell constructed within a filtered air lamina flow hood. This greatly reduced the possibility of contamination of the samples by ambient atmospheric and laboratory particles. Soot or kaolinite particles were deposited on a hydrophobic glass slide (the bottom surface of the flow cell) using the following technique. The dry soot or kaolinite particulates were placed in a glass vessel immersed in an ultrasonic bath. A flow of N_2 (99.999%) was passed through the glass vessel, and vibrations from the ultrasonic bath caused the dry particles to be suspended in the flow of N_2. This flow was then directed at the hydrophobic glass slide, and the soot or kaolinite particles were deposited on the slide by impaction. Soot agglomerates or kaolinite particles deposited on the substrate were always less than 40 μm in diameter. The optical resolution limit of our microscope was ~1 μm. A typical sample held between 200 to 800 individual particles, a majority of which were between 1 and 20 μm in diameter. Shown in Figure 2 is an image of a typical soot sample recorded prior to a deposition freezing experiment.

[11] The flow cell was located on a cooling stage. The temperature of the cooling stage and hence the flow cell was regulated with a refrigerating circulator (Thermo Neslab RTE-740). An insulating spacer, made from polychlorotrifluoroethylene (PCTFE), was placed between the hydrophobic glass slide and the flow cell body. This ensured that the coldest portion of the flow cell was the glass substrate (by ~10 K), thus preventing unwanted ice nucleation in other parts of the cell. All seals within the cell were made with Viton O-rings.

[12] A flow of humidified gas was introduced to one side of the cell and exited on the other where its frost point was measured with a frost point hygrometer (General Eastern). From the frost point measurements, the water vapor pressure (P_{H2O}) was calculated using the parameterization of *Marti and Mauersberger* [1993] which is in excellent agreement with the more rigorous equations from *Murphy and Koop* [2005] over our frost point range. A flow of humidified gas was generated by passing a flow of He (99.999%) over a reservoir of ultrapure water (distilled water was further purified using a millipore system). The desired P_{H2O} was adjusted by altering the temperature of the water reservoir and diluting the humidified flow with a second flow of dry He. A continuous and constant flow of between 1900 to 2100 cm^3 min^{-1} (at 273.15 K and 1 atm) was maintained throughout the course of the experiment. The He gas used in these experiments was first passed through a trap containing molecular sieves (1/16″ pellets, Type T4A) at 77 K and then through a 0.02 μm filter (Anodisc 25).

[13] A Pt-100 resistance temperature detector (RTD) from Omega was embedded within the aluminum base to measure the temperature of the bottom surface of the cell. The RTD was calibrated against the dew point or ice frost point within the cell, as done previously [*Middlebrook et al.*, 1993; *Parsons et al.*, 2004b]. To do this water droplets or ice crystals (depending on the temperature) were allowed to nucleate and grow on the bottom substrate, by slowly decreasing the temperature of the cell. Then the cell temperature was slowly (rate = 0.1 K min^{-1}) ramped up until the water droplets or ice crystals were observed to shrink (depending on whether water or ice particles were present). Next the cell temperature was slowly decreased again until the water droplets/ice crystals started to grow. From these observations we determined the temperature at which water droplets or ice crystals were in equilibrium

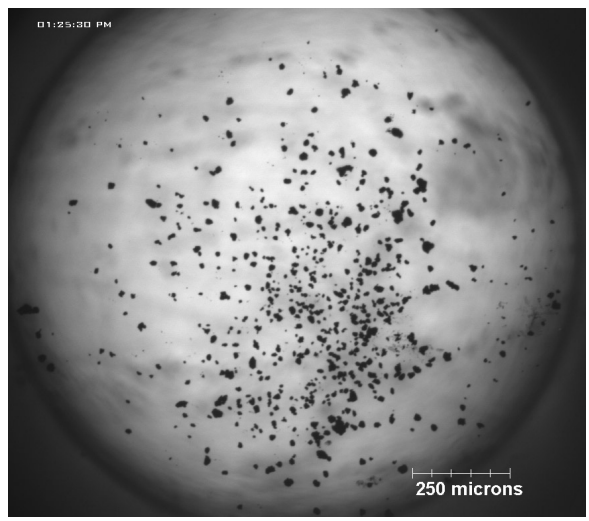

Figure 2. Image of a typical soot sample recorded prior to a deposition freezing experiment.

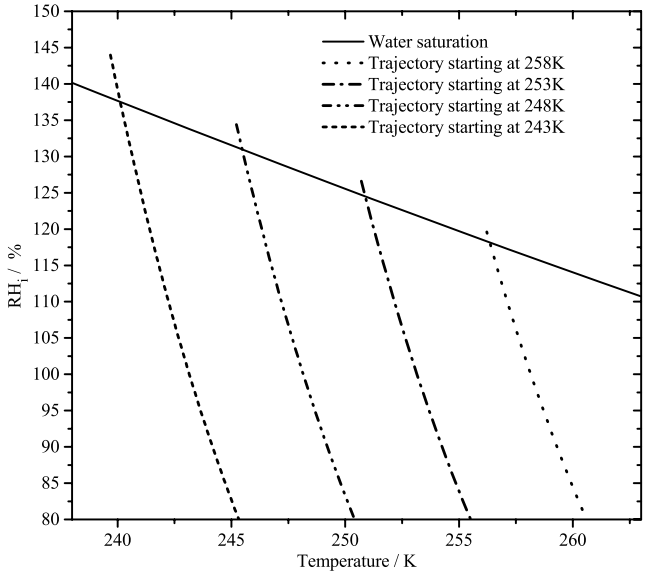

Figure 3. Typical experimental trajectories of RH_i, where temperature was reduced at a rate of 0.1 K min^{-1}, while the water partial pressure was constant. The trajectories were calculated using the saturation vapor pressure of water from *Koop et al.* [2000] and the saturation vapor pressure of ice from *Marti and Mauersberger* [1993].

with the gas-phase water vapor. At this point the temperature of the bottom surface of the cell was equal to the dew point or ice frost point of the vapor (again depending on whether water or ice particles were present), which was determined independently from the hygrometer measurements. (The hygrometer measurements gave the ice frost point, but this could be converted into a dew point using the saturation vapor pressure of water from *Koop et al.* [2000] and the saturation vapor pressure of ice from *Marti and Mauersberger* [1993].) The size of the water droplets or ice crystals was accurately determined from the digitally recorded images. By ramping the temperature of the cell up and down, the offset for the RTD was accurately determined for each experiment.

[14] The RH_i within the cell was calculated with the following equation:

$$RH_i = \frac{P_{H2O}}{P_{ice}(T_{cell})} \quad (1)$$

where $P_{ice}(T_{cell})$ is the saturation vapor pressure of ice at the temperature of the bottom surface of the flow cell. $P_{ice}(T_{cell})$ was calculated using the parameterization of *Marti and Mauersberger* [1993], and P_{H2O} was calculated as discussed above.

[15] In most nucleation experiments, the RH_i was ramped from below 100% to water saturation by decreasing the temperature of the cell at 0.1 K min^{-1}, and maintaining a constant P_{H2O} inside the cell. Typical experimental RH_i trajectories are illustrated in Figure 3 for four different initial temperatures of 258 K, 253 K, 248 K, and 243 K. For the remainder of the document these experiments will be referred to as RH_i ramp experiments. Images of the soot or clay particles were recorded digitally every 10 s or $\sim$0.017 K, while simultaneously P_{H2O} and the cell temperature were recorded. From the images we determined the RH_i at which water droplets or ice particles first formed in our experiments (i.e., the onset of water or ice nucleation).

[16] As mentioned above we also examined the ice nucleating properties of Lamp Black 101 after controlled exposes to O_3. Lamp Black 101 particles were deposited on a hydrophobic glass cover slide and exposed to O_3 within a flow tube in which $[O_3]$ was measured with a downstream chemical ionization mass spectrometer (CIMS). The flow tube and CIMS instrument have been described by *Knopf et al.* [2005]. In these experiments, the pressure of N_2 in the flow tube was 2–4 Torr and O_3 was generated by photolysis of O_2 at 254 nm. The following ozone exposures ($P_{O3}t$) were used: 1.6×10^{-3}, 7.6×10^{-3}, 13.0×10^{-3}, 25.1×10^{-3}, 35.6×10^{-3}, 94.8×10^{-3} atm s. This is equivalent to exposing the soot to 80 ppb of O_3 at atmospheric pressure for 0.2, 1.1, 1.9, 3.6, 5.1, and 13.7 days respectively. An O_3 concentration of 80 ppb at atmospheric pressure corresponds to relatively polluted conditions [*Finlayson-Pitts and Pitts*, 2000].

[17] We also carried out nucleation experiments with long observation times and at constant RH_i in order to constrain, as much as possible, the heterogeneous nucleation rate coefficient of ice on soot in the deposition mode (see below for a further discussion). For the remainder of the document we will refer to these experiments as constant RH_i experiments. In these experiments we employed n-hexane soot (air/fuel ratio = 2.4). As mentioned above, the International Steering Committee for Black Carbon Reference Materials has recommended using n-hexane in atmospheric studies. In the constant RH_i experiments, the temperature of the particles was held at $\sim$248 K, while the relative humidity was held at 124 ± 4% RH_i, which is just below water saturation. The particles were held at these conditions for an extended period of time (approximately 8 hours) and were monitored to determine if ice nucleated during this long observation time.

3. Results and Discussion

3.1. RH_i Ramp Experiments

[18] As mentioned above, P_{H2O} was held constant while the temperature of the cell was reduced in order to increase the RH_i within the flow cell. The temperature was decreased until either water droplets or ice particles were observed. The RH_i at which we observed either water droplets or ice particles are illustrated in Figure 4 for the blank hydrophobic glass slide as well as the different soot samples. The data points correspond to when we first observed either water or ice (in other words either the onset of water or ice formation). The error bars associated with the data points were calculated from the uncertainties of P_{H2O} and $P_{ice}(T_{cell})$, which resulted from the uncertainty in the dew point measurements and the calibration of temperature of the bottom surface of the flow cell. The dashed lines in Figure 4 represent water saturation (i.e., relative humidity with respect to water is 100%). The open symbols indicate that water droplets were first observed, and the solid symbols indicate that only ice particles were observed with no indication of the formation of water droplets prior to ice formation. From this information we make conclusions on

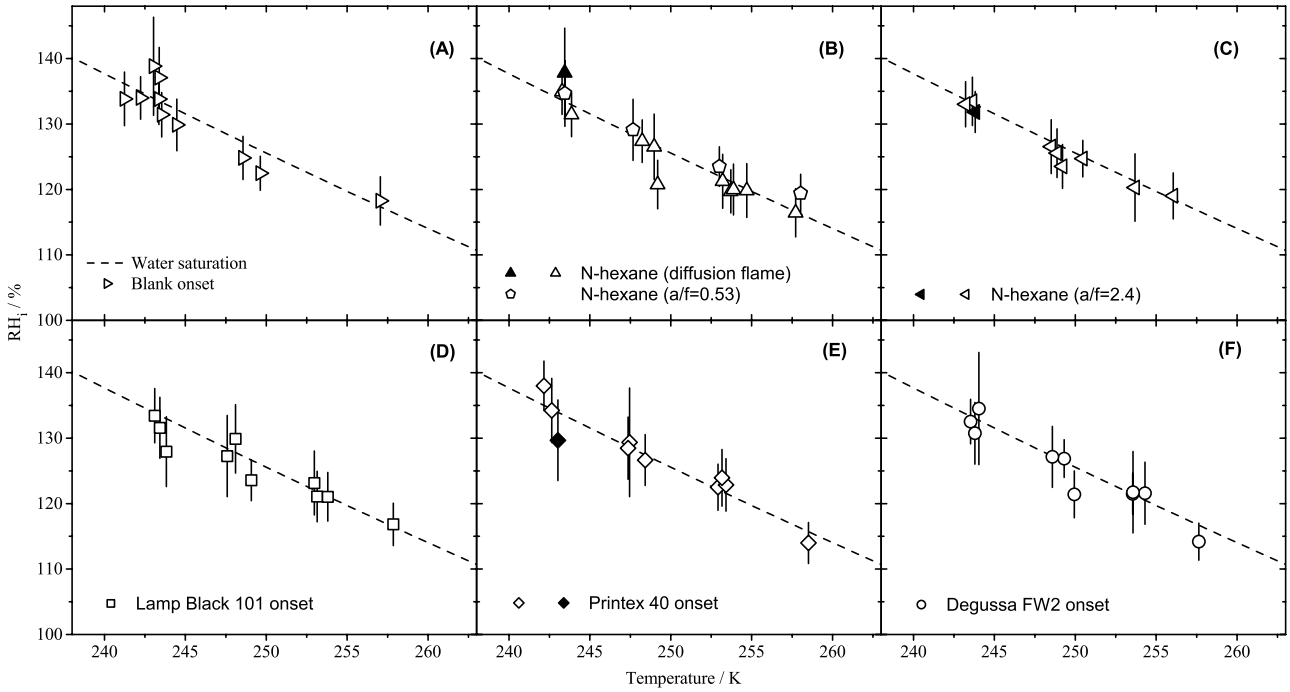

Figure 4. RH_i at which liquid water droplets or ice particles were first observed as the RH_i inside the cell was slowly increased. The open symbols indicate that water droplets were first observed, and the solid symbols indicate that only ice particles were observed with no indication of the formation of water droplets prior to ice formation. (a) Results from a control experiment, where no particles were deposited on the hydrophobic substrate. (b–f) Results from the six soot types listed in Table 1. The error bars associated with the data points were calculated from the uncertainties of P_{H2O} and $P_{ice}(T_{cell})$.

the ice nucleating ability of soot in the deposition mode below water saturation only (see below). In the experiments where water droplets were first observed (open symbols), ice nucleation would occasionally occur at a later time. This occurred with both the blank as well as with soot particles. However, we cannot determine from our results if the formation of ice after the formation of liquid droplets was due to the soot particles or the substrate. Hence we do not draw conclusions on the ice nucleation ability of soot in the condensation or immersion mode from these experiments. Also note that we do not draw conclusions on the CCN ability of soot from these experiments.

[19] The results in Figure 4 show that at 248 K and above, water droplets, rather than ice, always appeared first in our experiments. This occurred at water saturation, as expected. From this we can conclude that ice nucleation never occurred at temperatures above 248 K and below water saturation for our experimental conditions (observation time and soot particle concentrations). If ice nucleation did occur, ice particles would rapidly grow and prevent the formation of water droplets at water saturation by depleting the water vapor. As shown in Table 1, we investigated soots with a range of volatilities and carbon-to-oxygen ratios. Since we observed the same results for all the different soots investigated, below water saturation and above 248 K, our results suggest that the volatility and carbon-to-oxygen ratio does not significantly influence ice formation in this regime.

[20] At around 243 K, ice particles occasionally formed in our experiments with no indication of the formation of water droplets prior to ice formation (a total of three times). However, in the few experiments where ice did form the RH_i was close to water saturation when ice nucleation was observed, suggesting water nucleation may have occurred first followed by ice nucleation during the condensation process. In other words, for the few experiments where ice did form we cannot rule out condensation freezing. In fact, at between 243 and 258 K all the results (including when ice nucleated first) clustered around water saturation, suggesting water saturation is a prerequisite for both water and ice nucleation.

[21] For the experiments where water droplets first formed, we estimated an upper limit to the deposition nucleation rate coefficient of ice on soot particles, below water saturation. This rate coefficient provides a quantitative measure of the ice nucleating ability, which may be used in modeling studies of ice formation in the atmosphere. On the basis of Poisson statistics, if ice nucleation did not occur during the course of an experiment, an upper limit to the heterogeneous nucleation rate coefficient, J_{het}^{up}, can be calculated with the following equation [*Biermann et al.*, 1996; *Koop et al.*, 1995, 1997]:

$$J_{het}^{up} = \frac{1}{\tau A_s} \ln\left[\frac{1}{1-x}\right] \quad (2)$$

where τ is the observation time, A_s is the total surface area available for heterogeneous nucleation, and x is the confidence level (95% was used). In our RH_i ramp experiments τ was approximately 60 s and A_s ranged from 1×10^5 to 4×10^5 μm^2. To calculate A_s we assumed a

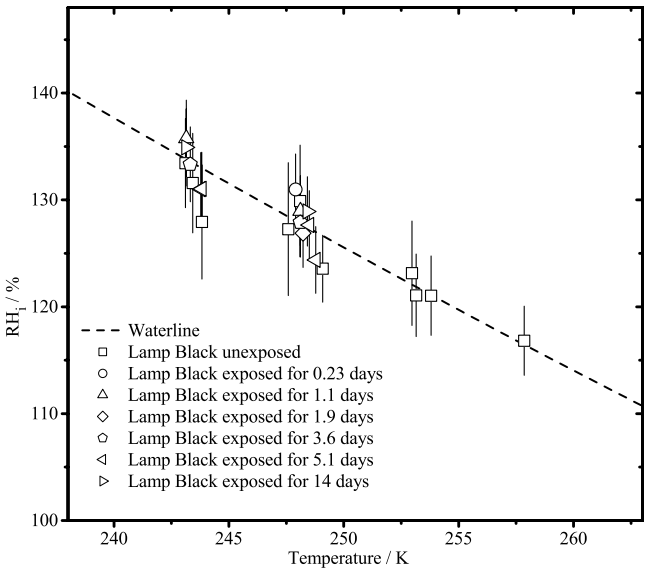

Figure 5. RH_i at which water droplets were observed for Lamp Black 101 soot samples treated with a range of O_3 exposures. In all experiments, water droplets were observed first (i.e., ice particles did not form unless water droplets first condensed). The exposure times indicated in the plot are equivalent atmospheric O_3 exposures at an atmospheric O_3 mixing ratio of 80 ppb (see text for details). The error bars associated with the data points were calculated from the uncertainties of P_{H2O} and $P_{ice}(T_{cell})$.

geometric surface area (= $4\pi r^2$, where r is the radius of the particles) for the soot particles. This is a conservative estimate as the surface area exposed to the gas phase is in most cases larger than the geometric surface area. On the basis of a surface area of 1×10^5 μm^2, J^{up}_{het} was calculated to be 50 cm^{-2} s^{-1}.

3.2. Ice Nucleation of Soot Particles Oxidized by O_3

[22] Lamp Black 101 was exposed to various amounts of ozone and then RH_i ramp experiments (constant ramp rate of 0.1 K min^{-1}) were performed to test the ice nucleation properties of these soots. The results are shown in Figure 5. The open symbols indicate that water droplets were observed first in all experiments. Also, the results for Lamp Black 101 exposed to ozone are the same as the results from unexposed Lamp Black 101. In all cases water droplets were first observed indicating that ice did not nucleate below water saturation. Even after an O_3 exposure of 9.5×10^{-2} atm s, which is equivalent to an exposure of 80 ppb at atmospheric pressure (polluted conditions) for 13.7 days, the results were not significantly different from results of unexposed Lamp Black 101. Either O_3 did not oxidize Lamp Black 101 significantly or the oxidation process did not change the IN ability significantly. Further research is needed to determine the extent of oxidation of Lamp Black 101 by O_3. Also more research is needed to determine if exposure to atmospherically relevant concentrations of ozone, as well as other atmospheric oxidants such as OH and NO_3 radicals, can modify the IN properties of other types of soot in the deposition mode as well as other modes of ice nucleation. These initial experiments show that exposure to atmospherically relevant concentrations of ozone did not modify the IN ability of Lamp Black 101 in the deposition mode below water saturation.

3.3. Comparison With Other Results

[23] As mentioned earlier there have been a few measurements of the ice nucleation ability of soot at temperatures above 238 K. In addition there have been a few studies at lower temperatures. *DeMott et al.* [1999] have investigated ice nucleation on Lamp Black 101 at temperatures ranging from 233 K to 213 K using a continuous flow diffusion chamber. In Figure 6, we compare these results with our data. At approximately 230 K, DeMott et al. observed ice nucleation only at water saturation. Hence, at warmer temperatures it is highly unlikely that they would observe ice nucleation below water saturation, which is consistent with our findings.

[24] *Möhler et al.* [2005a] investigated ice nucleation on spark generated soot at temperatures less than 240 K using a low-temperature aerosol and cloud chamber (AIDA). At temperatures between 235 K and 240 K, ice nucleation only occurred on uncoated soot particles after approaching water saturation. The authors commented that ice seems to form immediately in this temperature range after liquid activation of the soot particles either by condensation freezing or homogeneous freezing of the growing liquid water layer. This finding is consistent with our studies. More recently, *Möhler et al.* [2005b] used the AIDA chamber to investigate ice nucleation at low temperatures on soot produced from combustion of propane with various elemental carbon to

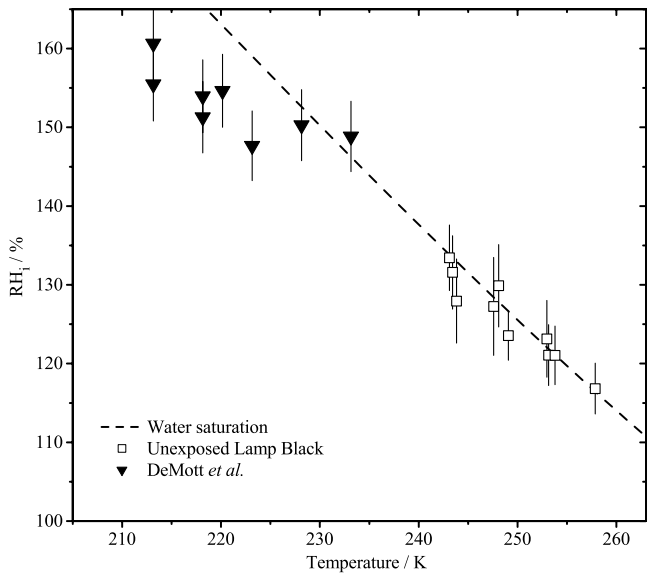

Figure 6. A comparison of our results for Lamp Black 101 (open squares) with those of *DeMott et al.* [1999] (solid triangles). Our data points correspond to the conditions at which water droplets were observed using soot particles ranging in size from 1 to 40 μm in diameter. In these experiments, water droplets were always observed first. If ice did form it was only after the appearance of water droplets. The results from DeMott et al. correspond to the onset for which 1% of Lamp Black soot particles (a number mean diameter of 240 nm) nucleated ice.

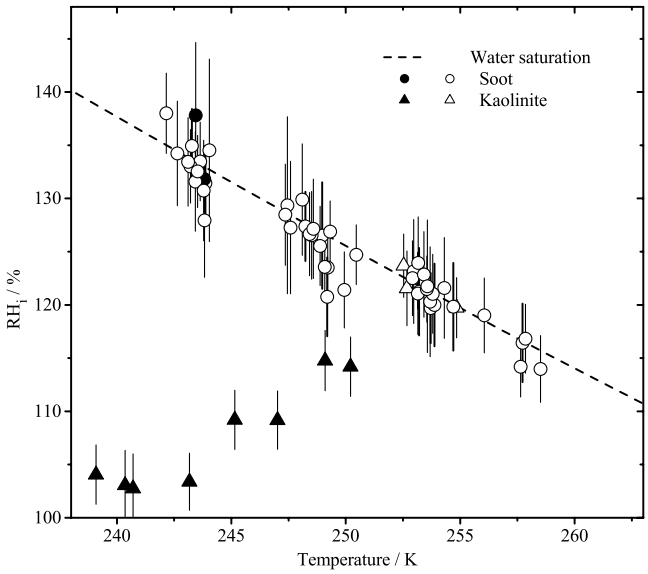

Figure 7. RH_i at which water droplets or ice particles were observed for soot and kaolinite experiments. The open symbols indicate that water droplets were first observed, and the solid symbols indicate that only ice particles were observed with no indication of the formation of water droplets prior ice formation. The error bars associated with the data points were calculated from the uncertainties of P_{H2O} and $P_{ice}(T_{cell})$.

organic carbon ratios. If these results are extrapolated to warmer temperatures they are also consistent with our findings.

[25] *DeMott* [1990] investigated ice nucleation on soot produced by combustion of acetylene at temperatures between 253 K and 233 K using an expansion cloud chamber. Because of the experimental design and experimental conditions, mainly condensation and immersion freezing were investigated. DeMott commented that there was some evidence of ice formation by deposition, but ice certainly did not precede cloud droplet formation by much. One of the conclusions from this study was that immersion freezing is an efficient ice nucleation process after water has condensed on soot particles.

[26] *Diehl and Mitra* [1998] investigated ice nucleation on soot produced by the combustion of kerosene. Combined deposition and condensation freezing (deposition/condensation freezing) were studied in a single experiment using a soap film method. Ice nucleation occurred in these experiments at temperatures as high as 253 K. In these experiments, the relative humidity was not measured, so a direct comparison with our results is difficult. All the deposition/condensation experiments may have been carried out slightly above water saturation and condensation freezing may have dominated. The authors also studied immersion freezing and contact freezing, and they found that kerosene-burner exhaust particles are effective ice nuclei in these freezing modes.

[27] Finally, *Gorbunov et al.* [2001] investigated soot produced by the combustion of benzene and toluene, as well as soot produced by thermal decomposition of benzene using a cloud chamber at temperatures ranging from 253 to 268 K. All experiments were carried out close to liquid water saturation: saturation with respect to liquid water was equal to 1.02 ± 0.02. It was found that the fraction of aerosol particles forming ice crystals was influenced by the concentration of surface chemical groups that can form hydrogen bonds with water molecules. A large difference in the ice-forming activity (3 orders of magnitude in the fraction of soot particles forming ice crystals) was observed for soot aerosols obtained with different generators. Soot particles produced by combustion of benzene and toluene were very potent ice nuclei, whereas soot produced by thermal decomposition of benzene were poor ice nuclei. They concluded that highly oxidized soot particles are extremely efficient ice nuclei. The difference between our results and the results from Gorbunov et al. may be due to a difference in experimental conditions: our research focuses on ice nucleation below water saturation and the work presented by Gorbunov et al. was carried out at or slightly above water saturation. Alternatively, the soot particles studied by Gorbunov et al. were more effective IN than the soot studied in our experiments.

[28] Combining all the previous results and those from our studies, it appears at temperatures above 243 K and below water saturation, ice nucleation on many types of soot particles are not efficient [*DeMott*, 1990; *DeMott et al.*, 1999; *Möhler et al.*, 2005a, 2005b]. In contrast, once the RH_i is above liquid water saturation, water can condense on soot particles, and then most types of soot may be important ice nuclei in the condensation or immersion mode [*DeMott*, 1990; *DeMott et al.*, 1999; *Diehl and Mitra*, 1998; *Gorbunov et al.*, 2001; *Möhler et al.*, 2005a, 2005b].

3.4. Ice Nucleation on Kaolinite

[29] As mentioned in the introduction, for comparison purposes we also investigated the ice nucleating ability of kaolinite particles. Kaolinite particles are believed to be a significant component of dust particles in the atmosphere [*Glaccum and Prospero*, 1980; *Pye*, 1987]. The results from this study are shown in Figure 7, along with all the results from soot experiments conducted in this study. In the kaolinite experiments we used a similar density of particles and particle sizes compared to our soot experiments, although the surface area available for nucleation is likely significantly higher in the soot experiments because of the large specific surface area of soot. Nevertheless, the RH_i values required for ice nucleation on kaolinite were significantly less than the RH_i values required for ice nucleation on soot particles. The results for kaolinite are generally consistent with previous measurements [*Bailey and Hallett*, 2002; *Roberts and Hallett*, 1968]. In a future publication we will focus on the IN ability of mineral dust particles including kaolinite.

3.5. Constant RH_i Experiments

[30] In the constant RH_i experiments, n-hexane soot particulates (air/fuel = 2.4) were held at 248 K and within 5% RH_i of water saturation (124 ± 4% RH_i) for approximately 8 hours. In this experiment the surface area of soot exposed to the vapor was 1.1×10^5 μm^2. Even during this long observation time at humidities close to water saturation, no ice was observed. From this we calculated an upper limit to the heterogeneous nucleation rate coefficient using

equation (2). In this case the upper limit to J_{het}^{up} was calculated to be 0.1 cm^{-2} s^{-1}. The upper limit is much smaller than the upper limit calculated from the RH_i ramp experiments, of 50 cm^{-2} s^{-1}, since the observation time was much longer (8 hours compared with 1 min). This allows us to provide a better constraint on the rate coefficient of ice nucleation in the deposition mode.

[31] From J_{het}^{up} calculated above we estimated the maximum number of ice particles that can be produced in the atmosphere at 248 K and at RH_i = 124%. The purpose is to place the magnitude of J_{het}^{up} determined experimentally into context. The following equation can be used to estimate the maximum number of ice particles that can be produced during a specified time period [*Pruppacher and Klett*, 1997],

$$n_{ice} = n_{soot}\left[1 - \exp\left(-J_{het}^{up} A_p \tau\right)\right] \quad (3)$$

where n_{ice} is the number density of ice particles produced (particles L^{-1}), n_{soot} is the number density of soot (L^{-1}), A_p is the surface area of a single soot particle (cm^2), and τ is the total time (seconds). For ice nucleation in the atmosphere we assumed τ was approximately 60 min, n_{soot} was 1.5×10^5 L^{-1}, and A_p was 1.3×10^{-9} cm^2. A value of 1.5×10^5 L^{-1} for n_{soot} was calculated by assuming a soot radius of 0.1 μm, a soot density of 2 g cm^{-3}, a geometric surface area for soot, and an elemental carbon mass concentrations in the atmosphere of approximately 1.3×10^{-6} g m^{-3} (which corresponds to urban-influenced rural areas [*Seinfeld and Pandis*, 1998; *Shah et al.*, 1986]). A value of 1.3×10^{-9} cm^2 for A_p was calculated on the basis of a geometric surface area and a soot radius of 0.1 μm. With these assumptions, a maximum number density of ice of 0.07 L^{-1} was obtained from equation (3). On the basis of field observations, *Meyers et al.* [1992] have developed empirical relationships between the number concentration of ice nuclei and ice supersaturation. This parameterization, which accounts for the combined effects of deposition nucleation and condensation freezing, predicts at 124% RH_i, the number of ice nuclei in the atmosphere is approximately 12 L^{-1}. Ice nucleation on soot particles below water saturation (with properties similar to the soot studied in our experiments and $n_{soot} = 1.5 \times 10^5$ L^{-1}) can only account for at most 0.6% of the ice nuclei density predicted by the Meyers et al. parameterization at 124% RH_i and 248 K.

4. Summary and Conclusions

[32] The ice nucleating properties of soot particles have been investigated in the deposition mode below water saturation. At 248 K and above, water droplets always nucleated first. From this we conclude that at these temperatures ice nucleation does not occur below water saturation under our experimental conditions. In the experiments where water droplets were first observed ice nucleation would occasionally occur at a later time. This occurred with both the blank as well as with soot particles. Hence we cannot determine from our results if the formation of ice after the formation of liquid droplets was due to the soot particles or the substrate. Below 248 K, ice occasionally formed in our experiments with no indication of the formation of water droplets prior to ice formation. However, even at these temperatures the RH_i was close to water saturation when ice nucleation was observed.

[33] The results of ice nucleation on Lamp Black 101 exposed to ozone were similar to the results from unexposed Lamp Black 101. Even after an O_3 exposure of 9.5×10^{-2} atm s, which is equivalent to an exposure of 80 ppb at atmospheric pressure for 13.7 days, the results were not significantly different from results of unexposed Lamp Black 101.

[34] Combining all the previous results and our studies, it appears that below water saturation at temperatures above 243 K, ice nucleation on many types of soot particles is not efficient [*DeMott*, 1990; *DeMott et al.*, 1999; *Möhler et al.*, 2005a, 2005b]. In contrast, once the RH_i is above liquid water saturation, water can condense on soot particles, and then most types of soot may be important ice nuclei in the condensation or immersion mode [*DeMott*, 1990; *DeMott et al.*, 1999; *Diehl and Mitra*, 1998; *Gorbunov et al.*, 2001; *Möhler et al.*, 2005a, 2005b].

[35] For comparison purposes we also investigated the IN ability of kaolinite particles. The results show that the ice nucleating ability of kaolinite in the deposition mode was superior to soot particles.

[36] We also carried out experiments with a constant RH_i and long observation times (8 hours) on n-hexane soot (air/fuel = 2.4). Even after a long observation time at close to water saturation, no ice was observed. From these measurements we calculated an upper limit to the heterogeneous nucleation rate coefficient of 0.1 cm^{-2} s^{-1} for a temperature of 248K and RH_i = 124 ± 4%. On the basis of this upper limit, if the number of soot particles in the atmosphere is 1.5×10^5 L^{-1}, then the number of ice particles produced below water saturation (and at these conditions) is at most 0.07 particles L^{-1}. In contrast, the parameterization by *Meyers et al.* [1992], which accounts for the combined effects of deposition nucleation and condensation freezing, predicts the number of ice nuclei in the atmosphere is approximately 12 L^{-1} at 124% RH_i. Hence we conclude that deposition nucleation of ice on soot particles cannot account for a significant proportion of the ice nuclei found in the Earth's troposphere above 243 K and below water saturation.

[37] **Acknowledgments.** The authors thank Dan Cziczo, Paul DeMott, and Boris Gorbonov for several helpful discussions regarding ice nucleation on soot. The authors also thank Dwight Smith for helpful discussions on the properties of soot as well as for providing us samples of n-hexane soot. This work was funded by the Canadian Foundation for Climate and Atmospheric Sciences (CFCAS), the Natural Science and Engineering Research Council of Canada (NSERC), and the Canada Foundation for Innovation (CFI).

References

Akhter, M. S., A. R. Chughtai, and D. M. Smith (1985), The structure of hexane soot-I - spectroscopic studies, *Appl. Spectrosc.*, *39*(1), 143–153.

Bailey, M., and J. Hallett (2002), Nucleation effects on the habit of vapour grown ice crystals from −18 to −42°C, *Q. J. R. Meteorol. Soc.*, *128*, 1461–1483.

Biermann, U. M., T. Presper, T. Koop, J. Mössinger, P. J. Crutzen, and T. Peter (1996), The unsuitability of meteoritic and other nuclei for polar stratospheric cloud freezing, *Geophys. Res. Lett.*, *23*(13), 1693–1696.

Choi, W., and M. T. Leu (1998), Nitric acid uptake and decomposition on black carbon (soot) surfaces: Its implications for the upper troposphere and lower stratosphere, *J. Phys. Chem. A*, *102*(39), 7618–7630.

Chughtai, A. R., J. M. Kim, and D. M. Smith (2002), The effect of air/fuel ratio on properties and reactivity of combustion soots, *J. Atmos. Chem.*, *43*(1), 21–43.

DeMott, P. J. (1990), An exploratory-study of ice nucleation by soot aerosols, *J. Appl. Meteorol.*, *29*(10), 1072–1079.
DeMott, P. J. (2002), Laboratory studies of cirrus cloud processes, in *Cirrus*, edited by D. K. Lynch et al., pp. 102–136, Oxford Univ. Press, New York.
DeMott, P. J., D. C. Rogers, and S. M. Kreidenweis (1997), The susceptibility of ice formation in upper tropospheric clouds to insoluble aerosol components, *J. Geophys. Res.*, *102*(D16), 19,575–19,584.
DeMott, P. J., Y. Chen, S. M. Kreidenweis, D. C. Rogers, and D. E. Sherman (1999), Ice formation by black carbon particles, *Geophys. Res. Lett.*, *26*(16), 2429–2432.
Diehl, K., and S. K. Mitra (1998), A laboratory study of the effects of a kerosene-burner exhaust on ice nucleation and the evaporation rate of ice crystals, *Atmos. Environ.*, *32*(18), 3145–3151.
Disselkamp, R. S., M. A. Carpenter, J. P. Cowin, C. M. Berkowitz, E. G. Chapman, R. A. Zaveri, and N. S. Laulainen (2000), Ozone loss in soot aerosols, *J. Geophys. Res.*, *105*(D8), 9767–9771.
Finlayson-Pitts, B. J., and J. N. Pitts Jr. (2000), *Chemistry of the Upper and Lower Atmosphere*, Elsevier, New York.
Gierens, K. (2003), On the transition between heterogeneous and homogeneous freezing, *Atmos. Chem. Phys.*, *3*, 437–446.
Glaccum, R. A., and J. M. Prospero (1980), Saharan aerosols over the tropical North Atlantic—Mineralogy, *Mar. Geol.*, *37*(3–4), 295–321.
Gorbunov, B., A. Baklanov, N. Kakutkina, H. L. Windsor, and R. Toumi (2001), Ice nucleation on soot particles, *J. Aerosol Sci.*, *32*(2), 199–215.
Heintzenberg, J. (1989), Fine particles in the global troposphere, *Tellus, Ser. B*, *41*, 149–160.
Intergovernmental Panel on Climate Change (2001), *Climate Change 2001: The Scientific Basis—Contributions of Working Group I to the Third Assessment Report of the Intergovernmental Panel on Climate Change*, edited by J.T. Houghton et al., 881 pp., Cambridge Univ. Press, New York.
Jensen, E. J., and O. B. Toon (1997), The potential impact of soot particles from aircraft exhaust on cirrus clouds, *Geophys. Res. Lett.*, *24*(3), 249–252.
Knopf, D. A., L. M. Anthony, and A. K. Bertram (2005), Reactive uptake of O_3 by multicomponent and multiphase mixtures containing oleic acid, *J. Phys. Chem. A*, *109*, 5579–5589.
Koop, T., U. M. Biermann, W. Raber, B. P. Luo, P. J. Crutzen, and T. Peter (1995), Do stratospheric aerosol droplets freeze above the ice frost point, *Geophys. Res. Lett.*, *22*(8), 917–920.
Koop, T., B. P. Luo, U. M. Biermann, P. J. Crutzen, and T. Peter (1997), Freezing of $HNO_3/H_2SO_4/H_2O$ solutions at stratospheric temperatures: Nucleation statistics and experiments, *J. Phys. Chem. A*, *101*(6), 1117–1133.
Koop, T., B. P. Luo, A. Tsias, and T. Peter (2000), Water activity as the determinant for homogeneous ice nucleation in aqueous solutions, *Nature*, *406*(6796), 611–614.
Lavanchy, V. M. H., H. W. Gaggeler, U. Schotterer, M. Schwikowski, and U. Baltensperger (1999), Historical record of carbonaceous particle concentrations from a European high-alpine glacier (Colle Gnifetti, Switzerland), *J. Geophys. Res.*, *104*(D17), 21,227–21,236.
Lohmann, U. (2002), A glaciation indirect aerosol effect caused by soot aerosols, *Geophys. Res. Lett.*, *29*(4), 1052, doi:10.1029/2001GL014357.
Lohmann, U., and J. Feichter (2005), Global indirect aerosol effects: A review, *Atmos. Chem. Phys.*, *5*, 715–737.
Marti, J., and K. Mauersberger (1993), A survey and new measurements of ice vapor-pressure at temperatures between 170 and 250 K, *Geophys. Res. Lett.*, *20*(5), 363–366.
Meyers, M. P., P. J. DeMott, and W. R. Cotton (1992), New primary ice nucleation parameterization in an explicit cloud model, *J. Appl. Meteorol.*, *31*, 708–721.
Middlebrook, A. M., L. T. Iraci, L. S. McNeill, B. G. Koehler, M. A. Wilson, O. W. Saastad, M. A. Tolbert, and D. R. Hanson (1993), Fourier transform-infrared studies of thin H_2SO_4/H_2O films: Formation, water uptake, and solid-liquid phase changes, *J. Geophys. Res.*, *98*(D11), 20,473–20,481.
Möhler, O., et al. (2005a), Effect of sulfuric acid coating on heterogeneous ice nucleation by soot aerosol particles, *J. Geophys. Res.*, *110*, D11210, doi:10.1029/2004JD005169.
Möhler, O., C. Linke, H. Saathoff, M. Schnaiter, R. Wagner, U. Schurath, A. Mangold, and M. Kramer (2005b), Ice nucleation on flame soot aerosol of different organic carbon content, *Meteorol. Z.*, *14*(4), 1–8.
Murphy, D. M., and T. Koop (2005), Review of the vapour pressures of ice and supercooled water for atmospheric applications, *Q. J. R. Meteorol. Soc.*, *131*(608), 1539–1565.
Pant, A., A. Fok, M. T. Parsons, J. Mak, and A. K. Bertram (2004), Deliquescence and crystallization of ammonium sulfate-glutaric acid and sodium chloride-glutaric acid particles, *Geophys. Res. Lett.*, *31*, L12111, doi:10.1029/2004GL020025.
Parsons, M. T., D. A. Knopf, and A. K. Bertram (2004a), Deliquescence and crystallization of ammonium sulfate particles internally mixed with water-soluble organic compounds, *J. Phys. Chem. A*, *108*(52), 11,600–11,608.
Parsons, M. T., J. Mak, S. R. Lipetz, and A. K. Bertram (2004b), Deliquescence of malonic, succinic, glutaric, and adipic acid particles, *J. Geophys. Res.*, *109*, D06212, doi:10.1029/2003JD004075.
Penner, J. E., M. O. Andreae, H. Annegarn, L. Barrie, J. Feichter, D. Hegg, A. Jayaraman, R. Leaitch, D. Murphy, and J. Nganga (2001), Aerosols, their direct and indirect effects, in *Climate Change 2001: The Scientific Basis—Contributions of Working Group I to the Third Assessment Report of the Intergovernmental Panel on Climate Change*, edited by J. T. Houghton et al., pp. 291–336, Cambridge Univ. Press, New York.
Pruppacher, H. R., and J. D. Klett (1997), *Microphysics of Clouds and Precipitation*, Springer, New York.
Pye, K. (1987), *Aeolian Dust and Dust Deposits*, Elsevier, New York.
Roberts, P., and J. Hallett (1968), A laboratory study of the ice nucleating properties of some mineral particulates, *Q. J. R. Meteorol. Soc.*, *94*, 25–34.
Seinfeld, J. H., and S. N. Pandis (1998), *Atmospheric Chemistry and Physics*, Wiley-Interscience, Hoboken, N. J.
Shah, J. J., R. L. Johnson, E. K. Heyerdahl, and J. J. Huntzicker (1986), Carbonaceous aerosol at urban and rural sites in the united states, *J. Air Pollut. Control Assoc.*, *36*, 254–257.
Tabor, K., L. Gutzwiller, and M. J. Rossi (1994), Heterogeneous chemical-kinetics of NO_2 on amorphous carbon at ambient temperature, *J. Phys. Chem.*, *98*(24), 6172–6186.
Vali, G. (1985), Nucleation terminology, *J. Aerosol Sci*, *16*, 575–576.
Vali, G. (1996), Ice nucleation—A review, in *Nucleation in Atmospheric Aerosols*, edited by M. Kulmala and P. Wagner, pp. 271–279, Elsevier, New York.

A. K. Bertram, M. Dymarska, M. L. Eastwood, D. A. Knopf, B. J. Murray, and L. Sun, Department of Chemistry, University of British Columbia, 2036 Main Mall, Vancouver, BC, Canada V6T 1Z1. (bertram@chem.ubc.ca)